Proceedings of the ASME 2018 International Mechanical Engineering Congress & Exposition
IMECE 2018
November 9-15, 2018, Pittsburgh, USA

IMECE2018-88294

COMPARISON OF INTERFACIAL AND CONTINUUM MODELS FOR DYNAMIC FRAGMENTATION ANALYSIS

Bahador Bahmani*
Mechanical, Aerospace,
& Biomedical Engineering Dept.
University of Tennessee, Knoxville
411 B.H. Goethert Pkwy
Tullahoma, Tennessee 37388
Email: bbahmani@vols.utk.edu

Philip Clarke
Mechanical, Aerospace,
& Biomedical Engineering Dept.
University of Tennessee, Knoxville
411 B.H. Goethert Pkwy
Tullahoma, Tennessee 37388
Email: pclarke1@utk.edu

Reza Abedi
Mechanical, Aerospace,
& Biomedical Engineering Dept.
University of Tennessee, Knoxville
411 B.H. Goethert Pkwy
Tullahoma, Tennessee 37388
Email: rabedi@utk.edu

ABSTRACT

The microstructural design has an essential effect on the fracture response of brittle materials. We present a stochastic bulk damage formulation to model dynamic brittle fracture. This model is compared with a similar interfacial model for homogeneous and heterogeneous materials. The damage models are rate-dependent, and the corresponding damage evolution includes delay effects. The delay effect provides mesh objectivity with much less computational efforts. A stochastic field is defined for material cohesion and fracture strength to involve microstructure effects in the proposed formulations. The statistical fields are constructed through the Karhunen-Loeve (KL) method. An advanced asynchronous Spacetime Discontinuous Galerkin (aSDG) method is used to discretize the final system of coupled equations. Application of the presented formulation is shown through dynamic fracture simulation of rock under a uniaxial compressive load. The final results show that a stochastic bulk damage model produces more realistic results in comparison with a homogenizes model.

1 INTRODUCTION

Brittle materials have a wide range of applications in various areas–from the geological application, such as rock, to biological applications, such as bone. The failure response of this kind of material is susceptible to a sudden rupture by initiation, propagation, and fragmentation of many cracks. The main reason of such a brittle rupture derives from the complex microstructure of these materials which consist of many microdefects and microcracks. The most challenging task in the numerical analysis of brittle materials is the modeling of fracture behavior. In the context of conventional continuum mechanics, there exist two frameworks for fracture modeling; *Interfacial* and *Bulk* models.

Interfacial models represent explicit sharp fractures in the computational domain. Three main models in this context are: the *linear elastic fracture mechanics* (LEFM) model, cohesive models [1, 2], and interfacial damage models [3–7]. Interfacial models explicitly track the real pattern of fractures, but their implementation is cumbersome and their computational cost is high. In applications such as multiscale methods, it is hard to track explicit discontinuities in all scales of interest. If it is even possible, the computation cost will be extremely high. However, the most important issue of these models is the need for additional criteria to predict the initiation and propagation direction of fractures.

Bulk models apply continuum damage mechanics to approximate the presence of explicit fractures with an implicit damage variable indicated the level of failure in an equivalent continuum domain. One of the earliest studies in this area refers to *Smeared Crack* approach in [8] where a continuum model is presented to simulate fractures in concrete. *Phase Field* approaches are the enhanced alternatives for bulk models [9–13]. Bulk models remedy the issues above in regard to fracture initiation, additional

*Address all correspondence to this author.

Copyright © 2018 by ASME

criteria for propagation direction, and challenges in fragmentation in interfacial models. Also, they provide several benefits from numerical aspects: Simple integration with other numerical methods, fast implementation, and straightforward utilization in multiscale analysis. The main drawback of bulk models is the overestimation of fracture sharpness which is much better handled by phase field approaches.

The effect of the microstructure is one of the important aspects of fracture response in quasi-brittle material. Al-Ostaz and Jasiuk [14] observed different fracture patterns in different samples with the same set-ups. The reason for this stochastic behavior is the high sensitivity of quasi-brittle materials to their microstructure defects. Similar observations are reported in [15], especially for responses after ultimate load capacity of the material when fractures are initiated and propagated. Another consequence of the high sensitivity of responses to microstructure is the *size effect* [16, 17]. One of the widely accepted models for studying the size effect is the Weibull's weakest link model. The efficiency of the Weibull method in capturing the size effect and statistical variation of fracture strength in interfacial models is shown in [18, 19]. We have used the Weibull model in the context of an interfacial damage model to capture statistical fracture response of rock, in hydraulic fracturing [20], fracture under dynamic compressive loading [21], and in fragmentation studies [7, 22]. However, these models are computationally expensive due to the use of a sharp interfacial model. In this study, we first use a random field approach, rather than the Weibull model, to represent material randomness. Second, in addition to a sharp damage model, we formulate a bulk damage model, where material cohesion is treated as a random field.

We will incorporate microstructural randomness in dynamic failure of brittle material through a stochastic approach. In the proposed stochastic approach, model parameters are constructed based on statistical fields. In the current study, we generate a realization of the statistical field for the fracture strength and material cohesion based on the well-known *Karhunen-Loève* (KL) method [23, 24]. In this regard, a recent study in [25] demonstrates the motivation of statistical models in high rates of loading in that the entire spatial domain fails in a short time period for problems that lack macroscopic stress concentration points.

The statistical damage formulation is coupled with elastodynamic equations for both the bulk and interfacial models. To solve these nonlinear systems of hyperbolic equations, we employ the *asynchronous Spacetime Discontinuous Galerkin* (aSDG) method; this method uses the Tent-Pitcher algorithm [26] to advance the solution by solving one patch (a small collection of elements) at a time until the computational spacetime domain is completely solved. This method results in a highly advanced numerical method with local and linear solution properties for the elastodynamic problem [27].

In the following sections, we will describe the proposed damage models, interfacial and bulk, and KL method in §2. We will show the effect of randomness and accuracy of the stochastic bulk model in §3 for a compressive sample to indicate the essential role of randomness in dynamics fracture analysis. Finally, we will discuss the novel contributions of this study in §4.

2 FORMULATION

In this section, we describe two different approaches for the modeling of brittle material failure. These approaches have the same origin from mathematical and physical aspects, but one represents the material failure as a localized/sharp phenomenon, and the other considers the failure mechanism as a bulk process in the material. After the description of the models, we will discuss a general method based on the KL method to involve stochastic effects into the introduced damage models.

Interfacial Model

The interfacial damage parameter D interpolated between the fully bonded ($D = 0$) to fully-debonded ($D = 1$) state on a contact/fracture interface. The macroscopic traction vector, $\mathbf{s}^*$, is given by,

$$\mathbf{s}^* = (1-D)\check{\mathbf{s}}_B + D\check{\mathbf{s}}_D \tag{1}$$

where $\check{\mathbf{s}}_B$ and $\check{\mathbf{s}}_D$ are dynamic Riemann solutions for bonded and debonded (separation, contact–stick, or contact–slip) modes. The formulas for these four states of Riemann solution are provided in [28]. The damage value is obtained by the evolution law,

$$\tau_c \dot{D} = D_{\text{src}}, \tag{2a}$$

$$D_{\text{src}} = 1 - e^{-a\langle D_{\text{frc}} - D\rangle_+}, \tag{2b}$$

$$D_{\text{frc}} = g(\check{s}, \check{\delta}), \tag{2c}$$

where $\dot{D}$ is the time derivative of D, τ_c is the time-scale or delay parameter, a is the brittleness factor, and $\langle . \rangle$ is the Macaulay positive operator. Similar to [29] we assume the damage evolution be driven by an effective stress $\check{s}$ and an effective separation $\check{\delta}$. In earlier works, *e.g.,* [7], damage is only driven by the effective traction, but as described in [29] the inclusion of $\check{\delta}$ is not only physically motivated but also improves the response of the model. Their definitions are motivated by the definition of effective scalar values in [30] and are given by,

$$\check{s} := \sqrt{\langle \check{s}_{\text{B}}^1 \rangle^2 + \beta_s^2 (\check{s}_{\text{B}}^2)^2} \tag{3a}$$

$$\check{\delta} := \sqrt{\langle \delta_1 \rangle^2 + \beta_\delta^2 \delta_2^2} \tag{3b}$$

Copyright © 2018 by ASME

where β_s and β_δ are traction and displacement mode-mixity coefficients, and $(\check{s}_{\mathrm{B}}^1, \check{s}_{\mathrm{B}}^2)$ and (δ_1, δ_2) are the normal and tangential components of bonded Riemann traction $\check{\mathbf{s}}_B$ and displacement jump (separation) vectors in 2D, respectively. The form of the function $g(\check{s}, \check{\delta})$ in Eqn. (2c) and the mode-mixity values for a Mohr-Coulomb model are provided in [29] and [21], respectively. The reader is also referred to [7] for a general discussion on this class of interfacial damage models and their comparison with conventional cohesive models.

Bulk Model

We use the same damage evolution law for the bulk model to provide a better comparison between the two models. The bulk model used in the current study is a nonlinear ordinary differential equation as,

$$\tau_c \dot{\kappa} = \kappa_{\mathrm{src}}, \tag{4a}$$

$$\kappa_{\mathrm{src}} = 1 - e^{-a\langle \kappa_{\mathrm{frc}} - \kappa \rangle}{}_+, \tag{4b}$$

$$\kappa_{\mathrm{frc}} = \frac{\sigma_r + \sigma_{\mathrm{ave}} \sin\phi}{c\cos\phi}, \tag{4c}$$

where $\dot{\kappa}$ is the time derivative of the damage variable κ, $0 \leq \kappa \leq 1$, c is the material cohesion, and ϕ is the friction angle. σ_{ave} and σ_r are the center and radius of the Mohr circle in the stress space, respectively. We define the damage force function, *i.e.,* κ_{frc}, based on the Mohr-Coulomb failure envelope. This definition is appropriate for brittle material with dominant failure modes in shear and tensile modes.

The proposed dynamics damage formulation, which is based on the Allix's formulation in [3, 31, 32], introduces a delay behavior into the damage mechanism through the time-scale parameter. The differences of our model and the Allix's formulation, particularly in relation to the definition of damage force Eqn. (4c) based on the Mohr-Coulomb failure criterion are further discussed in [33]. The delay effect of our model accounts for the non-instantaneous damage mechanism which is more consistent with the physical behavior of damage response in dynamic conditions. Also, the timescale τ_c preserves the mesh-objectivity of the aforementioned damage formulation by providing a non-local behavior in spacetime domain. This (temporal) non-local behavior and existence of an intrinsic length scale is required for bulk damage models [34] and is comparable with the spatial non-local characteristics in conventional gradient-based [35–37] and integration-based non-local [38] theories where they use a length-scale parameter. However, the delay method is preferable to those spatially non-local schemes due to its much less computational and implementation efforts.

We propose a damage-deformation relation by considering the effect of damage on deviatoric and hydrostatic tensile components of the elastic stress tensor as,

$$\boldsymbol{\sigma}_{\mathrm{eff}} = (1-\kappa)(\boldsymbol{\sigma}_d + \langle \boldsymbol{\sigma}_h \rangle) + (\boldsymbol{\sigma}_h - \langle \boldsymbol{\sigma}_h \rangle), \tag{5}$$

where $\boldsymbol{\sigma}_d$ and $\boldsymbol{\sigma}_h$ are deviatoric and hydrostatic parts of elastic stress tensor $\boldsymbol{\sigma}$.

Stochastic Field Realization

The uncertainty of a material property ξ is incorporated in the proposed damage models, bulk and interfacial, by treating a fracture strength parameter ξ as a spatially inhomogeneous random field $\xi(\mathbf{x}, \omega)$ governed by probability structure ω. The random field is developed by the imposition of a desired stationary covariance of γ-*exponential* form with a prescribed correlation length which controls the spatial variability of the field. A log-normal Lognormal(μ, σ^2) probability structure governs the distribution of the random field. This probability space has the mean $\exp\left(\mu + \sigma^2/2\right)$ and variance $[\exp(\sigma^2) - 1]\exp(2\mu + \sigma^2)$ of the log-normal field.

There exist several methods that allow a scalar random field approximation to be generated wherein the inherent statistics are preserved. One such method is the KL method which approximates the random field ξ by an expansion of its covariance kernel as the following series,

$$\xi(\mathbf{x}, \omega) = \mu_\xi(\mathbf{x}) + \sum_{i=1}^{n} \sqrt{\lambda_i} b_i(\mathbf{x}) Y_i(\omega), \tag{6}$$

where the eigenvalues λ_i and eigenfunctions $b_i(\mathbf{x})$ are extracted as solutions of the Fredholm equation, *i.e.,* the generalized eigenvalue problem (EVP), which is detailed in [39]. The truncated series with an appropriately chosen n number of terms can precisely represent the statics of the underlying random field, due to the monotonically decreasing property of the eigenvalue solutions. The series converges to the exact underlying statistics when $n \to \infty$, but the computation cost will be another factor to consciously choose the number of terms.

The uncorrelated random variables Y_i must also be independent for practical use of the KL method. This is valid only if the random variables and consequently the random field $\xi(\mathbf{x}, \omega)$ are Gaussian. This Gaussian requirement does not restrict the KL method robustness, since the *inverse transform method* provides a means of transforming one probability structure to another; this transformation needs *a prior* known cumulative density function of both distributions. Therefore, the KL Gaussian random field approximation is mapped to an approximation of the originally assumed log-normal distribution. Please refer to [40] for an overview of the use of KL method in modeling rock fracture strength and [22] for further elaboration on the KL and eigen-pair solution procedures, particularly for non-Gaussian fields.

Copyright © 2018 by ASME

3 NUMERICAL RESULTS

We investigate several aspects of the proposed models in fracture modeling of a brittle rock sample. Uniaxial compression tests in homogeneous and inhomogeneous conditions are studied. Figure 1 shows the geometry and boundary conditions of the studied problem. This plain strain specimen has the width and length of $w = 0.08$ m and $l = 2w = 0.16$ m, respectively.

Material properties are The rock material properties, listed in Tab. 1, are based on rock property groups discussed in [41]. The peak load and ramp time are fixed for all the following simulations which are $P_{\text{peak}} = 13.5$ MPa and $t_{\text{ramp}} = 0.01$ ms, respectively.

The computational domain in spacetime is discretized by simplicial tetrahedral elements, and the corresponding field unknowns, damage and displacement, are approximated by third-order basis functions in spacetime. We define a convergence criterion based on the energy norm of the coupled system, and the tolerance is 10^{-8}.

Density	ρ	2650 kg/m^3
Elastic modulus	E	65 GPa
Poisson ratio	ν	0.23
Cohesion	c	4.7 MPa
Friction angle	ϕ	17°
Time-scale parameter	τ_c	0.03
Brittleness factor	a	10

TABLE 1: MATERIAL PROPERTIES

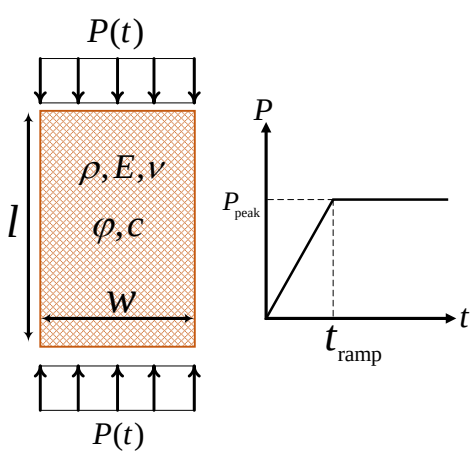

FIGURE 1: UNIAXIAL COMPRESSION TEST AND THE LOAD HISTORY.

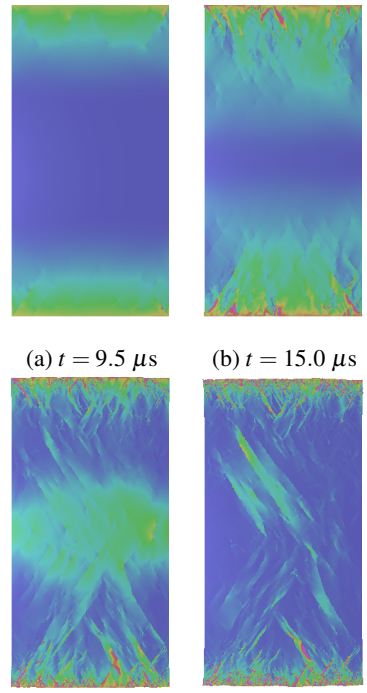

(a) $t = 9.5\ \mu$s (b) $t = 15.0\ \mu$s

(c) $t = 20.5\ \mu$s (d) $t = 26.0\ \mu$s

FIGURE 2: CRACK DISTRIBUTIONS AT VARIOUS TIMES IN THE INTERFACIAL MODEL WITH HOMOGENOUS PROPERTIES. THE COLOR FIELD SHOWS THE STRAIN ENERGY DENSITY ON THE DEFORMED GEOMETRY.

Homogeneous Material Property

In this section, we study failure mechanisms of the proposed bulk and interfacial models under the same boundary conditions and almost the same model parameters as listed in Tab. 1. Figures 2 and 3 show failure patterns for the interfacial and bulk models at different times, respectively. Although the responses are not well matched, the models have some similarities in some aspects. First, the initial damage zones are generated at specimen corners. Second, the fractures or damage zones propagate directionally toward the specimen center. However, there is a significant difference in the estimation of failure zones.

For both models the stress field is relatively uniform along the width of the domain as the wave propagates inward. The strength values are also uniform, due to using a homogeneous material mode. However, as seen in Fig. 2 for the interfacial model the fractures are localized rather than populating the entire width of the domain. This is explained by the interfacial nature of this model and small discretization errors; although the stress and strength fields are rather uniform, even small numerical errors cause certain points to be sites of crack nucleation. Subsequently, the stress field around these nucleation sites becomes highly nonuniform due to the stress concentration and

Copyright © 2018 by ASME

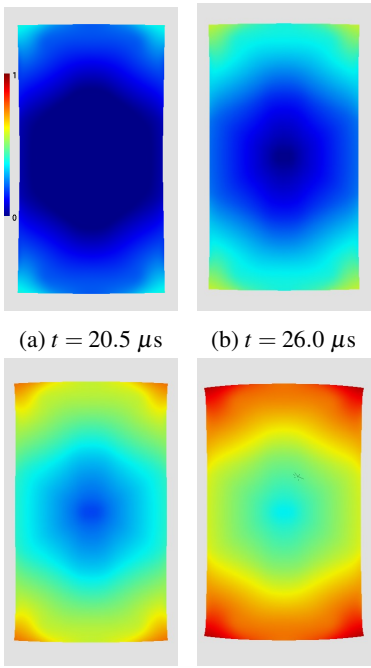

(a) $t = 20.5\ \mu s$ (b) $t = 26.0\ \mu s$

(c) $t = 31.5\ \mu s$ (d) $t = 37.0\ \mu s$

FIGURE 3: CONTOURS OF THE DAMAGE EVOLUTION AT DIFFERENT TIMES IN THE NON-ADAPTIVE BULK MODEL WITH HOMOGENEOUS PROPERTIES. THE DEFORMED MESHES ARE DEPICTED BY MAGNIFICATION FACTOR OF 250. COLORS FROM BLUE TO RED CORRESPOND TO BULK DAMAGE VALUES FROM ZERO TO ONE, RESPECTIVELY.

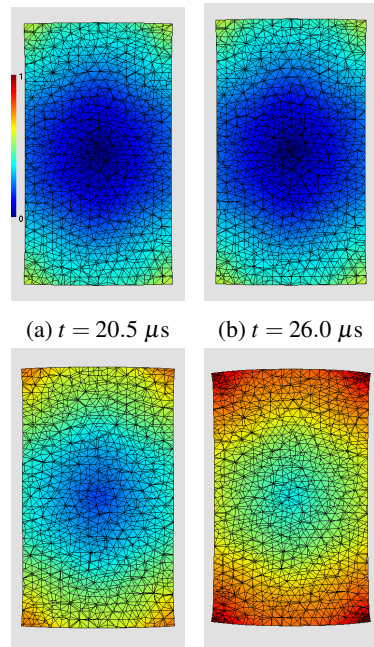

(a) $t = 20.5\ \mu s$ (b) $t = 26.0\ \mu s$

(c) $t = 31.5\ \mu s$ (d) $t = 37.0\ \mu s$

FIGURE 4: CONTOURS OF THE DAMAGE EVOLUTION AT DIFFERENT TIMES IN THE ADAPTIVE BULK MODEL WITH HOMOGENEOUS PROPERTIES. THE DEFORMED MESHES ARE DEPICTED BY MAGNIFICATION FACTOR OF 250. COLORS FROM BLUE TO RED CORRESPOND TO BULK DAMAGE VALUES FROM ZERO TO ONE, RESPECTIVELY.

shielded regions surrounding a propagating crack. The cracks are mostly along the angle $45^\circ - \phi/2 \approx 36.6^\circ$ with respect to the load orientation, which matches the predicted angle from the Mohr-Coulomb model [21]. On the other hand, for the bulk damage model fracture is rather uniform along the width of the domain, which does not match the localized failure zones observed experimentally.

This investigation has two outcomes: First, it shows the functionality of the adaptive method in the solution accuracy for tracking crack patterns in the interfacial model; second, it provides evidence of mesh insensitivity of the damage formulation which is a crucial problem in damage mechanics. Figure 4 depicts the application of the h-adaptive method in the bulk model. It is obvious there is not any improvement in the approximated failure zones, and the result is in an excellent agreement the result in Fig. 3 where the underlying mesh is a nonadaptive 32×64 structured grid of triangles. That is, the rather nonphysical distributed response of the bulk model is intrinsic; from its formulation and unlike the interfacial model, discretization errors and adaptive operations cannot induce localized failure zones.

Inhomogeneous Material Property

In this section, we show how the consideration of the material randomness results in more realistic responses of the bulk model. We consider random effects of the cohesion value in the bulk model and the tensile strength in the interfacial model. These material properties can significantly affect the failure response of the material as they control the initiation of the degradation process.

Figure 5 presents the KL realization of a random field with the correlation length of 5 mm, unitary mean value, and 25% variance for the standard normal form of the fracture strength field. This random distribution is used for the cohesion and fracture strength in the domain with the reported mean values in Tab. 1, *i.e.,* 4.7 MPa and 7 MPa, respectively. Other parameters are assumed homogeneous with the same previous values, and the boundary conditions are kept the same as before.

Figures 6 and 7 show the damage response and fracture propagation at different times for the interfacial and bulk models, respectively. The response of the bulk model indicates that weakest zones in the material have a dominant effect on the evolution

Copyright © 2018 by ASME

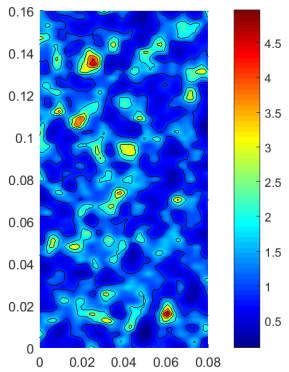

FIGURE 5: A KL REALIZATION WITH UNITARY MEAN AND 25% VARIANCE. THE CORRELATION LENGTH FOR THE RANDOM FIELD IS 5 mm.

of damage. This is concluded by the comparison of the initial damaged zones in Fig. 7a with weakest zones of the sample in Fig. 5. The randomness effect does not have any considerable contribution in the response of the interfacial model. This is due to two sources: First, interfacial models are localized, and so immediately they produce many stress concentration sites in the domain resulting in a localized response even for the homogeneous material strength case shown in Fig. 2; second, the compressive loading in the example is too high. Therefore the material does not have enough time to transfer the applied stresses to other places, and many cracks are generated immediately after the imposition of boundary loads. This statement is justifiable by the consideration of an infinite load. In such an extreme case the distribution of material property does not have any effect on the failure response, and the failure always occurs in the same regions. The other factor that may affect the interaction of randomness and the load amplitude is the confinement pressure in bi-axial compression tests which is not studied in this paper. Besides, as the employed damage model is rate-dependent, another crucial topic for further investigations is the interaction of length scales implied by the rate-dependent model and the random field for fracture strength. We leave these questions for future works.

The heterogeneity structure of the material cohesion significantly changes the bulk model response to a more realistic behavior. In Fig. 7, the damage initiates from the weakest points in the material instead of initiation from corners in Fig. 3. The most interesting outcome is the appropriate recovery of the failure zones in the bulk model results. These failure zones are more aligned with the top and bottom boundary edges which are in a good agreement with the interfacial model in Fig. 6d; instead of corners in Fig. 3d. Also, we see more localized behaviors in special directions after the generation of the initial damage spots which considerably modify the globally diffusive behavior in the previous homogeneous example. In compressible tests, these specific inclined failure zones are expected by the Mohr-Coulomb model, and the provided result is comparable with other numerical and experimental observations [42–46]. This example shows how the randomness improves the reality of the solutions and reduces computational cost with the simpler bulk model.

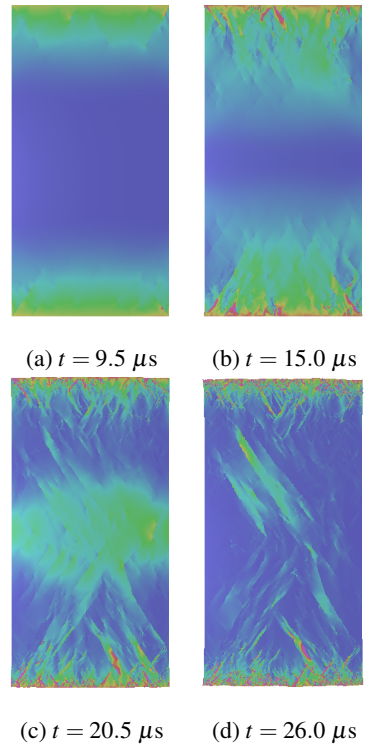

(a) $t = 9.5\ \mu s$ (b) $t = 15.0\ \mu s$

(c) $t = 20.5\ \mu s$ (d) $t = 26.0\ \mu s$

FIGURE 6: CRACK DISTRIBUTIONS AT VARIOUS TIMES IN THE INTERFACIAL MODEL WITH HETEROGENEOUS FRACTURE STRENGTH. THE COLOR FIELD SHOWS THE STRAIN ENERGY DENSITY ON THE DEFORMED GEOMETRY.

4 CONCLUSION

In the current study, we formulated a dynamic stochastic damage model for brittle failure. The introduced time-scale parameter in the damage model incorporates rate effects into this model and preserves the mesh objectivity. A statistical framework is formulated based on the KL expansion method to quantify material randomness in the stochastic bulk and interfacial models. We formulated an advanced numerical technology based on the aSDG method to solve the highly nonlinear coupled system of hyperbolic equations. The main advantage of this numerical method is to precisely track wave fronts in highly dynamic impact problems. The final system of nonlinear equations is solved with the Newton-Raphson method.

Copyright © 2018 by ASME

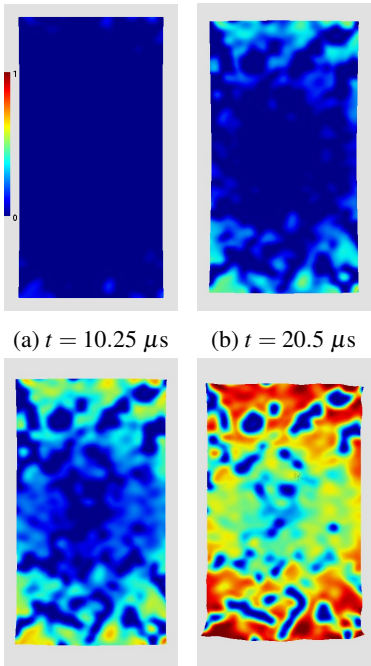

(a) $t = 10.25\ \mu$s (b) $t = 20.5\ \mu$s

(c) $t = 26.0\ \mu$s (d) $t = 37.0\ \mu$s

FIGURE 7: CONTOURS OF THE DAMAGE EVOLUTION AT DIFFERENT TIMES IN THE BULK MODEL WITH HETEROGENEOUS COHESION. THE DEFORMED MESHES ARE DEPICTED BY MAGNIFICATION FACTOR OF 250. COLORS FROM BLUE TO RED CORRESPOND TO BULK DAMAGE VALUES FROM ZERO TO ONE, RESPECTIVELY.

We showed the most critical factor to get more realistic responses from bulk models is the consideration of randomness effects. Although for this high amplitude loading problem the response of the interfacial model did not change considerably with random fracture strength, the response of the bulk model was significantly affected by a random cohesion field. Therefore, a homogeneous fracture strength field is not an appropriate alternative for bulk models for certain problems. The mesh objectivity of the proposed damage formulation is proven by a comparison between a fixed-mesh and h-adaptive refined mesh results.

In this work, we assumed an artificial statistics for corresponding random variables in the statistical analysis. In future works, we aim to use statistical volume elements (SVEs) to homogenize random properties of brittle material at different length scales. We will characterize fracture related parameters as random variables with load angle dependence similar to [47].

ACKNOWLEDGMENT

The authors gratefully acknowledge partial support for this work via the U.S. National Science Foundation (NSF), CMMI - Mechanics of Materials and Structures (MoMS) program grant number 1538332 and CCF - Scalable Parallelism in the Extreme (SPX) program grant number 1725555.

REFERENCES

[1] Dugdale, D. S., 1960. "Yielding of steel sheets containing slits". *Journal of the Mechanics and Physics of Solids,* ***8***, pp. 100–104.

[2] Barenblatt, G. I., 1962. "The mathematical theory of equilibrium of cracks in brittle fracture". *Advanced Applied Mechanics,* ***7***, pp. 55–129.

[3] Allix, O., Feissel, P., and Thévenet, P., 2003. "A delay damage mesomodel of laminates under dynamic loading: basic aspects and identification issues". *Computers & structures,* ***81***(12), pp. 1177–1191.

[4] Alfano, G., 2006. "On the influence of the shape of the interface law on the application of cohesive-zone models". *Composites Science and Technology,* ***66***(6), pp. 723–730.

[5] Parrinello, F., Failla, B., and Borino, G., 2009. "Cohesive-frictional interface constitutive model". *International Journal of Solids and Structures,* ***46***(13), pp. 2680 – 2692.

[6] Nguyen, V. P., 2014. "Discontinuous galerkin/extrinsic cohesive zone modeling: Implementation caveats and applications in computational fracture mechanics". *Engineering Fracture Mechanics,* ***128***, pp. 37–68.

[7] Abedi, R., Haber, R. B., and Clarke, P. L., 2017. "Effect of random defects on dynamic fracture in quasi-brittle materials". *International Journal of Fracture,* ***208***(1-2), pp. 241–268.

[8] Bažant, Z. P., and Lin, F. B., 1988. "Nonlocal smeared cracking model for concrete fracture". *Journal of Structural Engineering,* ***114***(11), pp. 2493–2510.

[9] Francfort, G., and Marigo, J.-J., 1998. "Revisiting brittle fracture as an energy minimization problem". *Journal of the Mechanics and Physics of Solids,* ***46***(8), pp. 1319 – 1342.

[10] Bourdin, B., Francfort, G., and Marigo, J.-J., 2000. "Numerical experiments in revisited brittle fracture". *Journal of the Mechanics and Physics of Solids,* ***48***(4), pp. 797 – 826.

[11] Miehe, C., Welschinger, F., and Hofacker, M., 2010. "Thermodynamically consistent phase-field models of fracture: Variational principles and multi-field fe implementations". *International Journal for Numerical Methods in Engineering,* ***83***(10), pp. 1273–1311.

[12] Borden, M. J., Hughes, T. J., Landis, C. M., and Verhoosel, C. V., 2014. "A higher-order phase-field model for brittle fracture: Formulation and analysis within the isogeometric

Copyright © 2018 by ASME

analysis framework". *Computer Methods in Applied Mechanics and Engineering,* ***273***, pp. 100–118.

[13] Klinsmann, M., Rosato, D., Kamlah, M., and McMeeking, R. M., 2015. "An assessment of the phase field formulation for crack growth". *Computer Methods in Applied Mechanics and Engineering,* ***294***, pp. 313–330.

[14] Al-Ostaz, A., and Jasiuk, I., 1997. "Crack initiation and propagation in materials with randomly distributed holes". *Engineering Fracture Mechanics,* ***58***(5-6), pp. 395–420.

[15] Kozicki, J., and Tejchman, J., 2007. "Effect of aggregate structure on fracture process in concrete using 2D lattice model". *Archives of Mechanics,* ***59***(4-5), pp. 365–84.

[16] Rinaldi, A., Krajcinovic, D., and Mastilovic, S., 2007. "Statistical damage mechanics and extreme value theory". *International Journal of Damage Mechanics,* ***16***(1), pp. 57–76.

[17] Genet, M., Couegnat, G., Tomsia, A., and Ritchie, R., 2014. "Scaling strength distributions in quasi-brittle materials from micro- to macro-scales: A computational approach to modeling nature-inspired structural ceramics". *Journal of the Mechanics and Physics of Solids,* ***68***(1), pp. 93–106.

[18] Weibull, W., 1939. "A statistical theory of the strength of materials". *R. Swed. Inst. Eng. Res.*, p. Res. 151.

[19] Weibull, W., 1951. "A statistical distribution function of wide applicability". *Journal of Applied Mechanics,* ***18***, pp. 293–297.

[20] Abedi, R., Omidi, O., and Clarke, P., 2016. "Numerical simulation of rock dynamic fracturing and failure including microscale material randomness". In Proceeding: 50th US Rock Mechanics/Geomechanics Symposium. ARMA 16-0531.

[21] Abedi, R., Haber, R., and Elbanna, A., 2017. "Mixed-mode dynamic crack propagation in rocks with contact-separation mode transitions". In Proceeding: 51th US Rock Mechanics/Geomechanics Symposium. ARMA 17-0679.

[22] Clarke, P., Abedi, R., Bahmani, B., Acton, K., and Baxter, S., 2017. "Effect of the spatial inhomogeneity of fracture strength on fracture pattern for quasi-brittle materials". In Proceedings of ASME 2017 International Mechanical Engineering Congress & Exposition IMECE 2017, p. V009T12A045 (9 pages). IMECE2017-71515.

[23] Karhunen, K., and Selin, I., 1960. *On linear methods in probability theory*. Rand Corporation.

[24] Loéve, M., 1977. *Probability theory*. Springer, New York.

[25] Abedi, R., Omidi, O., and Clarke, P., 2017. "A numerical study on the effect of loading and randomness on fracture patterns in a tight formation". In Proceeding: 51th US Rock Mechanics/Geomechanics Symposium. ARMA 17-0641.

[26] Abedi, R., Chung, S.-H., Erickson, J., Fan, Y., Garland, M., Guoy, D., Haber, R., Sullivan, J. M., Thite, S., and Zhou, Y., 2004. "Spacetime meshing with adaptive refinement and coarsening". In Proceedings of the Twentieth Annual Symposium on Computational Geometry, SCG '04, ACM, pp. 300–9.

[27] Abedi, R., Haber, R. B., and Petracovici, B., 2006. "A spacetime discontinuous Galerkin method for elastodynamics with element-level balance of linear momentum". *Computer Methods in Applied Mechanics and Engineering,* ***195***, pp. 3247–73.

[28] Abedi, R., and Haber, R. B., 2014. "Riemann solutions and spacetime discontinuous Galerkin method for linear elastodynamic contact". *Computer Methods in Applied Mechanics and Engineering,* ***270***, pp. 150–77.

[29] Abedi, R., Omidi, O., and Clarke, P., June 25-28, 2017. "A numerical study on the effect of loading and randomness on fracture patterns in a tight formation". In Proceeding: 51th US Rock Mechanics/Geomechanics Symposium.

[30] Camacho, G. T., and Ortiz, M., 1996. "Computational modelling of impact damage in brittle materials". *International Journal of Solids and Structures,* ***33***, pp. 2899–2938.

[31] Allix, O., and Corigliano, A., 1999. "Modeling and simulation of crack propagation in mixed-modes interlaminar fracture specimens". *International Journal of Fracture,* ***38***, pp. 111–140.

[32] Corigliano, A., and Ricci, M., 1999. "Rate-dependent interface models: formulation and numerical applications". *International Journal of Solids and Structures,* ***38***, pp. 547–576.

[33] Bahmani, B., Clarke, P. L., and Abedi, R., 2018. "A bulk damage model for modeling dynamic fracture in rock". In Proceeding: 52nd US Rock Mechanics/Geomechanics Symposium. ARMA 18-151-0228-0826 (10 pages).

[34] Peerlings, R., De Borst, R., Brekelmans, W., and Geers, M., 2002. "Localisation issues in local and nonlocal continuum approaches to fracture". *European Journal of Mechanics, A/Solids,* ***21***(2), pp. 175–89.

[35] Lasry, D., and Belytschko, T., 1988. "Localization limiters in transient problems". *International Journal of Solids and Structures,* ***24***(6), pp. 581–597.

[36] Peerlings, R., De Borst, R., Brekelmans, W., and De Vree, J., 1996. "Gradient enhanced damage for quasi-brittle materials". *International Journal for Numerical Methods in Engineering,* ***39***(19), pp. 3391–403.

[37] Thai, T. Q., Rabczuk, T., Bazilevs, Y., and Meschke, G., 2016. "A higher-order stress-based gradient-enhanced damage model based on isogeometric analysis". *Computer Methods in Applied Mechanics and Engineering,* ***304***, pp. 584–604.

[38] Pijaudier-Cabot, G., and Bažant, Z. P., 1987. "Nonlocal damage theory". *Journal of engineering mechanics,* ***113***(10), pp. 1512–1533.

[39] Ghanem, R., and Spanos, P., 1991. *Stochastic finite elements: a spectral approach*. Springer-Verlag.

[40] Clarke, P., and Abedi, R., 2017. "Fracture modeling of

Copyright © 2018 by ASME

rocks based on random field generation and simulation of inhomogeneous domains". In Proceeding: 51th US Rock Mechanics/Geomechanics Symposium. ARMA 17-0643.

[41] Hoek, E., 2000. "Practical rock engineering".

[42] Tang, C., Tham, L., Lee, P., Tsui, Y., and Liu, H., 2000. "Numerical studies of the influence of microstructure on rock failure in uniaxial compression - part II: constraint, slenderness, and size effect". *International Journal of Rock Mechanics and Mining Sciences,* ***37***(4), pp. 571–583.

[43] Teng, J., Zhu, W., and Tang, C., 2004. "Mesomechanical model for concrete. part ii: applications". *Magazine of Concrete Research,* ***56***(6), pp. 331–345.

[44] Li, G., and Tang, C.-A., 2015. "A statistical meso-damage mechanical method for modeling trans-scale progressive failure process of rock". *International Journal of Rock Mechanics and Mining Sciences,* ***74***, pp. 133–150.

[45] Dinç, Ö., and Scholtès, L., 2017. "Discrete analysis of damage and shear banding in argillaceous rocks". *Rock Mechanics and Rock Engineering*, pp. 1–18.

[46] Rangari, S., Murali, K., and Deb, A., 2018. "Effect of meso-structure on strength and size effect in concrete under compression". *Engineering Fracture Mechanics*.

[47] Acton, K. A., Baxter, S. C., Bahmani, B., Clarke, P. L., and Abedi, R., 2018. "Voronoi tessellation based statistical volume element characterization for use in fracture modeling". *Computer Methods in Applied Mechanics and Engineering,* ***336***, pp. 135–155.

Copyright © 2018 by ASME